AMERICAN SOCIETY FOR MICROBIOLOGY | Molecular and Cellular Biology®

RESEARCH ARTICLE

Obesity-Linked Phosphorylation of SIRT1 by Casein Kinase 2 Inhibits Its Nuclear Localization and Promotes Fatty Liver

Sung E. Choi,[a,b] Sanghoon Kwon,[a] Sunmi Seok,[a] Zhen Xiao,[c] Kwan-Woo Lee,[d] Yup Kang,[b] Xiaoling Li,[e] Kosaku Shinoda,[f] Shingo Kajimura,[f] Byron Kemper,[a] Jongsook Kim Kemper[a]

Department of Molecular and Integrative Physiology, University of Illinois at Urbana-Champaign, Urbana, Illinois, USA[a]; Department of Physiology, Ajou University School of Medicine, Suwon, Kyunggi-do, Republic of Korea[b]; Laboratory of Proteomics and Analytical Technologies, Frederick National Laboratory for Cancer Research, Frederick, Maryland, USA[c]; Department of Endocrinology and Metabolism, Ajou University School of Medicine, Suwon, Kyunggi-do, Republic of Korea[d]; Laboratory of Signal Transduction, National Institute of Environmental Health Sciences, Research Triangle Park, North Carolina, USA[e]; Laboratory UCSF Diabetes Center and Department of Cell and Tissue Biology, University of California, San Francisco, San Francisco, California, USA[f]

ABSTRACT Sirtuin1 (SIRT1) deacetylase delays and improves many obesity-related diseases, including nonalcoholic fatty liver disease (NAFLD) and diabetes, and has received great attention as a drug target. SIRT1 function is aberrantly low in obesity, so understanding the underlying mechanisms is important for drug development. Here, we show that obesity-linked phosphorylation of SIRT1 inhibits its function and promotes pathological symptoms of NAFLD. In proteomic analysis, Ser-164 was identified as a major serine phosphorylation site in SIRT1 in obese, but not lean, mice, and this phosphorylation was catalyzed by casein kinase 2 (CK2), the levels of which were dramatically elevated in obesity. Mechanistically, phosphorylation of SIRT1 at Ser-164 substantially inhibited its nuclear localization and modestly affected its deacetylase activity. Adenovirus-mediated liver-specific expression of SIRT1 or a phosphor-defective S164A-SIRT1 mutant promoted fatty acid oxidation and ameliorated liver steatosis and glucose intolerance in diet-induced obese mice, but these beneficial effects were not observed in mice expressing a phosphor-mimic S164D-SIRT1 mutant. Remarkably, phosphorylated S164-SIRT1 and CK2 levels were also highly elevated in liver samples of NAFLD patients and correlated with disease severity. Thus, inhibition of phosphorylation of SIRT1 by CK2 may serve as a new therapeutic approach for treatment of NAFLD and other obesity-related diseases.

KEYWORDS deacetylase, NAFLD, steatosis, diabetes, fatty acid oxidation, PGC-1alpha, sirtuin

Received 5 January 2017 **Returned for modification** 28 January 2017 **Accepted** 5 May 2017

Accepted manuscript posted online 22 May 2017

Citation Choi SE, Kwon S, Seok S, Xiao Z, Lee K-W, Kang Y, Li X, Shinoda K, Kajimura S, Kemper B, Kemper JK. 2017. Obesity-linked phosphorylation of SIRT1 by casein kinase 2 inhibits its nuclear localization and promotes fatty liver. Mol Cell Biol 37:e00006-17. https://doi.org/10.1128/MCB.00006-17.

Address correspondence to Jongsook Kim Kemper, jongsook@illinois.edu.

S. E. Choi, S. Kwon, and S. Seok contributed equally to this study.

Obesity is a rapidly growing global epidemic and substantially increases the risk for diabetes, nonalcoholic fatty liver disease (NAFLD), and many other metabolic disorders (1). More than 80% of obese patients have NAFLD, which can progress to steatohepatitis (NASH) and further to end-stage liver diseases, such as fibrosis, cirrhosis, and liver cancer (2, 3), but good therapeutic options for NAFLD and diagnostic markers for monitoring disease progression are not available. The hallmark of NAFLD is abnormal accumulation of triglycerides (TGs) in the liver, partly due to perturbations in hepatic lipid metabolism (2, 3). Mounting evidence from pharmacological and genetic studies has established that sirtuin1 (SIRT1) is a key regulator of hepatic lipid metabolism and prevents and improves the symptoms of NAFLD and many other obesity-related diseases (4–8).

SIRT1 is an NAD^+-dependent deacetylase that functions as a master energy sensor

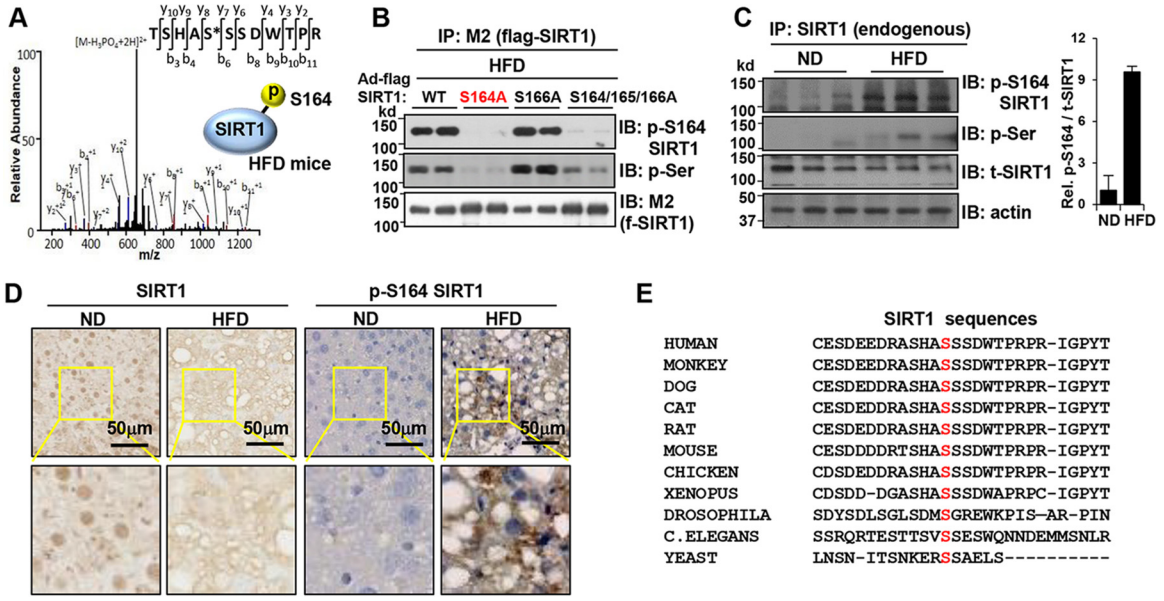

FIG 1 Identification of obesity-related phosphorylation of SIRT1 at S164. (A) Mice fed an ND or HFD were infected with Ad-Flag-SIRT1 or control Ad-GFP virus, and Flag-SIRT1 was isolated and subjected to LC-MS/MS analysis. S164 was identified with high confidence as a phosphorylation site only in HFD mice. (B) SIRT1-WT or its mutants, S164A, S166A, and S164/165/166A, were adenovirally expressed in mice fed an HFD, and 1 week later, levels of p-S164–SIRT1 or Ser-phosphorylated SIRT1 in whole-cell liver extracts were detected by IP/IB (n = 2 mice). (C) Phosphorylation of endogenous SIRT1 in livers of HFD mice (n = 3 mice) was detected by IP/IB using either p-S164-specific SIRT1 antibody or pan-p-Ser antibody. At the right, levels of p-S164–SIRT1 were quantified. (D) Endogenous SIRT1 and p-S164–SIRT1 in liver sections of mice fed an ND or HFD were detected by IHC. (E) Alignment of sequences adjacent to S164-SIRT1 (hS172), which is highlighted in red, in different species.

and mediates homeostatic transcriptional responses (5, 6, 9). SIRT1 deacetylates and modulates activities of many gene-regulatory proteins, including PGC-1α and SREBP-1, and activates gluconeogenesis and fatty acid oxidation and inhibits lipogenesis during fasting (10–12). Treatment with natural or synthetic SIRT1 activators (STACs) (13, 14) or supplements increasing cellular NAD^+ levels (15–17) improved insulin sensitivity and metabolic outcomes in diabetic obese mice. Further, genetic or virus-mediated liver-specific expression of SIRT1 (12, 18) prevented NAFLD and ameliorated fatty liver symptoms, and conversely, liver-specific deletion of SIRT1 attenuated fat oxidation and increased inflammation (19). SIRT1 function is aberrantly low in obese animals, so understanding the mechanisms for the low SIRT1 function is important for development of therapeutic drugs for treating NAFLD and other obesity-related diseases.

In this study, we show that SIRT1 is aberrantly phosphorylated at S164 in fatty livers of diet-induced obese mice by casein kinase 2 (CK2), the expression of which is dramatically increased in obesity. We show that this phosphorylation inhibits nuclear localization with modest effects on the deacetylase activity of SIRT1, inhibits fatty acid oxidation, and promotes pathological symptoms of NAFLD. We further show that levels of phosphorylation of SIRT1 and CK2 are highly elevated in liver specimens of NAFLD patients and are correlated with disease severity.

RESULTS

Identification of S164 as an obesity-linked SIRT1 phosphorylation site. To identify obesity-linked posttranslational modifications (PTMs) of SIRT1 that could affect its function, Flag-mouse SIRT1 was adenovirally (Ad) expressed in livers of mice that had been fed a normal chow diet (ND) or a high-fat diet (HFD). Flag-SIRT1 in liver extracts was isolated and SIRT1 PTMs were identified by an unbiased proteomic liquid chromatography-tandem mass spectrometry (LC-MS/MS) analysis. Multiple potential PTM sites were identified in SIRT1, and phosphorylated S164 (human Ser-172) was detected with the highest confidence only in the HFD obese mice (Fig. 1A).

First, to determine if S164 is a major Ser phosphorylation site in SIRT1 in obese mice, wild-type SIRT1 (SIRT1-WT) and S164A-SIRT1, S166A-SIRT1, or S164/165/166A mutants

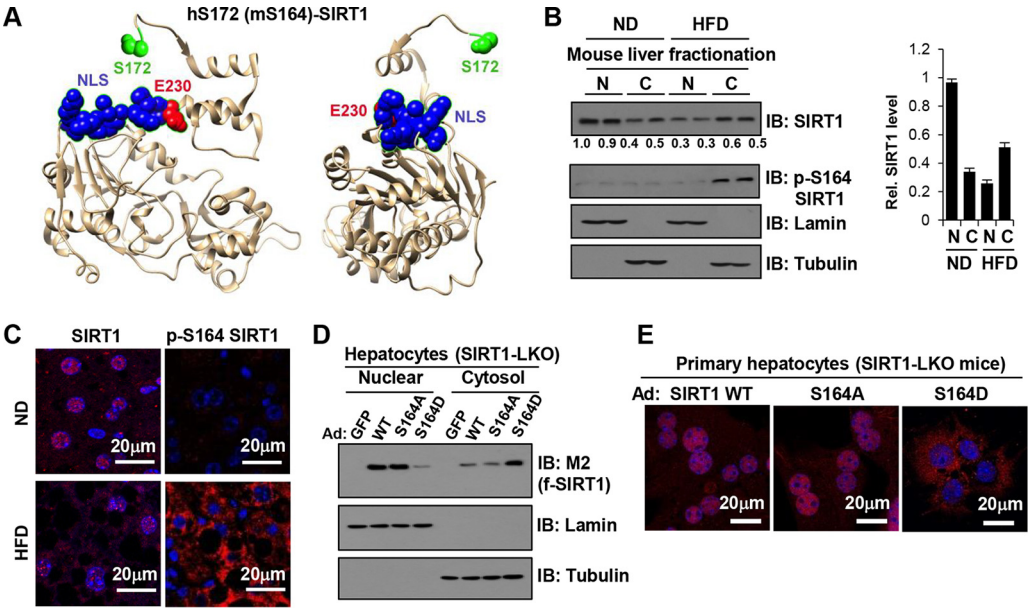

FIG 2 S164-SIRT1 phosphorylation inhibits its nuclear localization. (A) Illustration of the locations of S172 (mS164), E230 (mE222), and NLS2 in human SIRT1. The structure of human SIRT1 from residues 174 to 658 (Protein Data Bank entry 5BTR) is shown. For illustration purposes, Ser-Ser has been added at the N terminus to represent S172 and S173. The image on the right has been rotated 90° relative to that on the left. (B) Levels of endogenous SIRT1 and p-S164–SIRT1 in cytoplasmic (C) and nuclear (N) fractions were detected in duplicate by IB from mice fed an ND or HFD. Relative (Rel.) levels for each sample are shown below the blot, and the averages are plotted at the right. (C) Endogenous SIRT1 and p-S164–SIRT1 in liver sections of mice fed an ND or HFD were detected by IF. (D and E) SIRT1-WT, S164A-SIRT1, or S164D-SIRT1 was adenovirally expressed in hepatocytes from SIRT1-LKO mice, and the subcellular localization of SIRT1 was examined by biochemical fractionation (D) and IF (E) studies.

were adenovirally expressed in HFD obese mice, and p-Ser SIRT1 levels in liver extracts were measured. Mutation of S164A or S164/165/166A led to marked decreases in phosphorylated Ser levels in SIRT1 and levels of SIRT1 phosphorylated specifically at S164, detected by pan-Ser or the p-S164 antibodies, respectively, whereas mutation of S166A did not (Fig. 1B). The substantial decrease in phosphorylation detected by the pan-Ser antibody suggests that S164 is a major phosphorylation site, but other Ser residues may be phosphorylated and the pan-Ser antibody may not detect all phosphorylated Ser.

Phosphorylation both specifically at S164 (p-S164) and at serine residues of endogenous SIRT1 was substantially increased in HFD-induced obese mice (Fig. 1C). Further, in immunohistochemical (IHC) analysis of liver sections of ND or HFD mice, endogenous p-S164–SIRT1 levels, detected by the p-S164–SIRT1-specific antibody, were substantially increased in mice fed an HFD (Fig. 1D). Remarkably, S164 in mouse SIRT1 is highly conserved among species from yeast to human (Fig. 1E), suggesting the functional importance of this residue. This *in vivo* proteomic analysis and biochemical studies indicate that SIRT1 is phosphorylated at S164 in diet-induced obese mice.

Obesity-linked phosphorylation of SIRT1 at S164 inhibits its nuclear localization. Based on the structure of human SIRT1 (20), mouse mS164 (hS172) is located near the m223-230 (h231-238) nuclear localization sequence (21) and mE222 (hE230), which is critical for SIRT1 activation by all reported STACs, including resveratrol and SRT1720 (13) (Fig. 2A). The N-terminal domain of SIRT1 plays a critical role in the binding of SIRT1 to STACs and SIRT1-interacting proteins, such as AROS and PACS-2, resulting in allosteric modulation of its deacetylase activity (22–24). Thus, we examined the effects of S164 phosphorylation on the nuclear localization and the deacetylation activity of SIRT1.

Since p-S164–SIRT1 levels are substantially elevated in diet-induced obese mice (Fig. 1), we first examined the effects of an HFD on subcellular localization of SIRT1. Levels of SIRT1 in nuclear fractions were substantially decreased, and remarkably, p-S164–

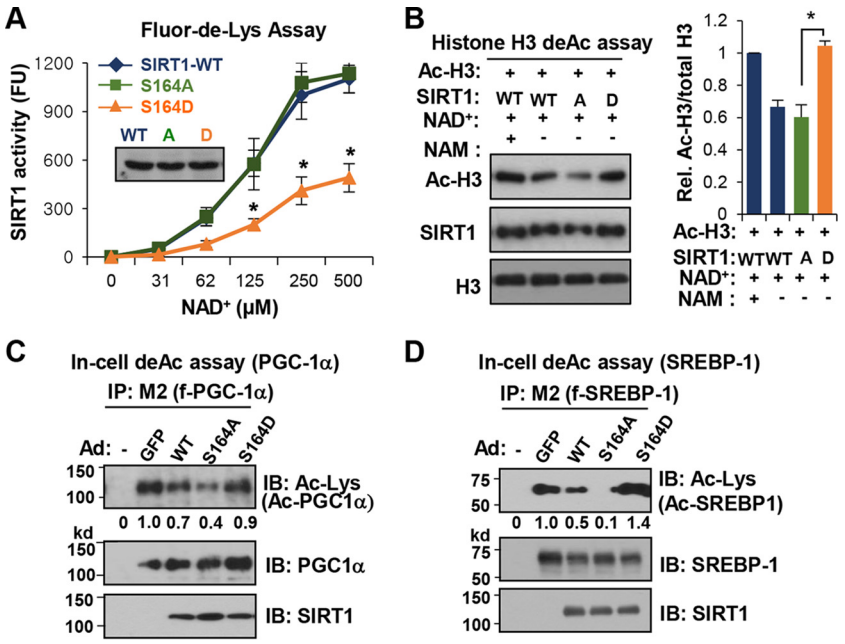

FIG 3 S164-SIRT1 phosphorylation inhibits its deacetylase activity. (A) Flag-SIRT1-WT, S164A-SIRT1, and S164D-SIRT1 were expressed in Cos-1 cells. Fluorescently labeled Ac-p53 peptide was incubated with Flag-SIRT1 proteins that were immunoprecipitated from whole-cell extracts, and SIRT1 deacetylase activity was measured as described in Materials and Methods. Results are shown as standard errors of the means (SEM) ($n = 3$); *, P value of <0.05 for Ad-SIRT(S164A) versus Ad-SIRT1 (164D). (B) Flag-SIRT1 proteins bound to M2 agarose were incubated with acetylated histone H3 *in vitro*, in the presence of NAD^+ and an inhibitor of SIRT1, nicotinamide (NAM), as indicated, and levels of acetylated histone H3 and input proteins were detected by IB (SEM [$n = 3$]; *, P value of <0.05 for Ad-SIRT1 [164A] versus Ad-SIRT1 [164D]). Statistical significance was determined by one-way ANOVA with Tukey's test. (C and D) In-cell deacetylation assays. Cos-1 cells were transfected with plasmids as indicated, and acetylated levels of PGC-1α (C) and SREBP-1 (D) were measured by IP/IB. Relative amounts are indicated below the blot. Consistent results were observed from two independent deacetylation assays.

SIRT1 was detected only in the cytoplasm of HFD mice (Fig. 2B). Consistent with these results, in immunofluorescence (IF) studies, SIRT1 was detected mostly in the nucleus in ND mice but was predominantly in the cytoplasm in HFD mice with reduced expression, while p-S164–SIRT1 levels were highly elevated in the HFD mice and restricted to the cytoplasm (Fig. 2C). To further examine the effect of S164 phosphorylation on nuclear localization of SIRT1, SIRT1-WT, phosphor-defective S164A-SIRT1, or phosphor-mimic S164D-SIRT1 was expressed in hepatocytes from SIRT1-liver-specific knockout (LKO) mice. SIRT1-WT and S164A-SIRT1 were mostly in the nucleus, whereas S164D-SIRT1 was mainly in the cytoplasm, as detected by subcellular fractionation (Fig. 2D) and immunofluorescence (Fig. 2E). These results demonstrate that phosphorylation of S164 in SIRT1 inhibits its nuclear localization.

Phosphorylation of SIRT1 at S164 inhibits its deacetylase activity. We next determined the effect of mutation of S164 on the deacetylase activity of SIRT1. SIRT1 deacetylase activity was assayed utilizing a fluorescently labeled substrate, acetylated p53 (Ac-p53) peptide. Deacetylase activity of the p-mimic S164D mutant was decreased compared to that of the SIRT1-WT or the p-defective S164A mutant (Fig. 3A). Similarly, in histone deacetylation assays *in vitro*, Ac-histone H3 levels were decreased by incubation with SIRT1-WT or the S164A mutant but not with the S164D mutant (Fig. 3B). These results suggest that the intrinsic deacetylase activity of SIRT1 is reduced by phosphorylation at S164.

PGC-1α and SREBP-1 are well-known targets of SIRT1 and play critical roles in transcriptional regulation of hepatic lipid metabolism (10–12, 19). Deacetylation of PGC-1α by SIRT1 increases the transcriptional activity of PGC-1α and promotes mitochondrial biogenesis and fatty acid oxidation, and conversely, deacetylation of SREBP-1

inhibits the activity of SREBP-1 and decreases lipogenesis. In Cos-1 cells, levels of Ac-PGC-1α and Ac-SREBP-1 were decreased by expression of SIRT1-WT and more markedly decreased by expression of S164A-SIRT1, while acetylated protein levels were not decreased by expression of phosphor-mimic S164D-SIRT1 (Fig. 3C and D). These results suggest that S164 phosphorylation of SIRT1 in cells inhibits its function, possibly in part by decreasing its deacetylase activity, in addition to inhibiting its nuclear localization.

Obesity-induced CK2 mediates phosphorylation of SIRT1 at S164. The CK2 motif, S/TXXE/D, was the most highly predicted protein kinase motif containing S164 in SIRT1 using the KinasePhos and Scan Site programs. CK2 is a constitutively active Ser/Thr kinase and interacts with its target proteins through acidic amino acid clusters (25, 26). Notably, an acidic amino acid cluster, 153-ESDDDDRTS-162, is located near S164 in SIRT1 in mice and other vertebrates (Fig. 1E).

To determine if CK2 mediates the obesity-induced S164 phosphorylation of SIRT1, the effects of a CK2 inhibitor or short interfering RNA (siRNA) downregulation of CK2 on phosphorylation of SIRT1 were examined in hepatocytes treated with cytokines to mimic elevated proinflammatory cytokine levels that are observed in obesity (27). Treatment with interleukin-1β (IL-1β) most markedly increased S164-SIRT1 phosphorylation levels (Fig. 4A). Phosphorylation of SIRT1 in IL-1β-treated hepatocytes was dramatically reduced by treatment with a CK2 inhibitor, 4,5,6,7-tetrabromobenzotriazole (TBB) but not by inhibitors of ERK, JNK, and p38 (Fig. 4B), and downregulation of CK2 by two different siRNA sequences led to substantial decreases in p-S164–SIRT1 levels (Fig. 4C). Consistent with these results, in *in vitro* kinase assays, CK2 phosphorylated SIRT1-WT but not S164A-SIRT1 (Fig. 4D). Further, in glutathione *S*-transferase (GST) pulldown assays, CK2 directly interacts with SIRT1 through its N-terminal domain, which contains the acidic amino acid cluster (Fig. 4E).

We further examined whether interaction of SIRT1 and CK2 was altered in obesity. In coimmunoprecipitation (CoIP) assays, the interaction of these two proteins was detected only in HFD mice (Fig. 4F). Both SIRT1-WT or the p-defective S164A mutant coimmunoprecipitated with CK2 (Fig. 4G), suggesting that S164 phosphorylation is not required for the interaction with CK2. CK2 and p-S164 SIRT1 are located nearly exclusively in the cytoplasm in HFD mice in IF analysis (Fig. 4H). Remarkably, CK2 expression is dramatically increased, whereas SIRT1 expression is decreased, in livers of HFD mice (Fig. 4F and I). Protein levels of CK2 were increased over 25-fold in mice fed an HFD compared to ND-fed mice, whereas mRNA levels of CK2 increased only about 2- to 3-fold (Fig. 4I). Consistent with these results, IL-1β treatment of hepatocytes increased protein and mRNA levels of CK2 about 20-fold and 3- to 4-fold, respectively (Fig. 4J). It was shown that in adipose tissue, CK2 is induced by cold exposure through cyclic AMP (cAMP) signaling (28). Similarly, treatment with an activator of PKA/cAMP signaling, forskolin (Fsk), increased CK2 mRNA levels about 2-fold and increased protein levels about 10-fold (Fig. 4J). These results suggest that expression of CK2 is increased in mouse liver in response to an HFD, primarily at the level of posttranslational regulation, and the increase correlates with dramatically increased levels of p-S164–SIRT1 in the cytoplasm.

Since the p-mimic Asp mutation at S164 reduced the intrinsic activity of SIRT1 (Fig. 3A), we tested if CK2 phosphorylation affects the deacetylation activity of SIRT1. Incubation of immunoprecipitated Flag-SIRT1 from Cos-1 nuclear extracts with CK2 *in vitro* resulted in increased phosphorylation of SIRT1 at S164 and a small but statistically significant decrease in SIRT1 activity in *in vitro* deacetylation assays (Fig. 4K). The decrease was less than that observed with S164D-SIRT1 (Fig. 3A) but is an underestimate, since there is some phosphorylation of SIRT1 in the Cos-1 cells (Fig. 4K) and it is unlikely that 100% of SIRT1 molecules are phosphorylated by CK *in vitro*. These results suggest that CK2-mediated phosphorylation of SIRT1 modestly inhibits the intrinsic activity of SIRT1.

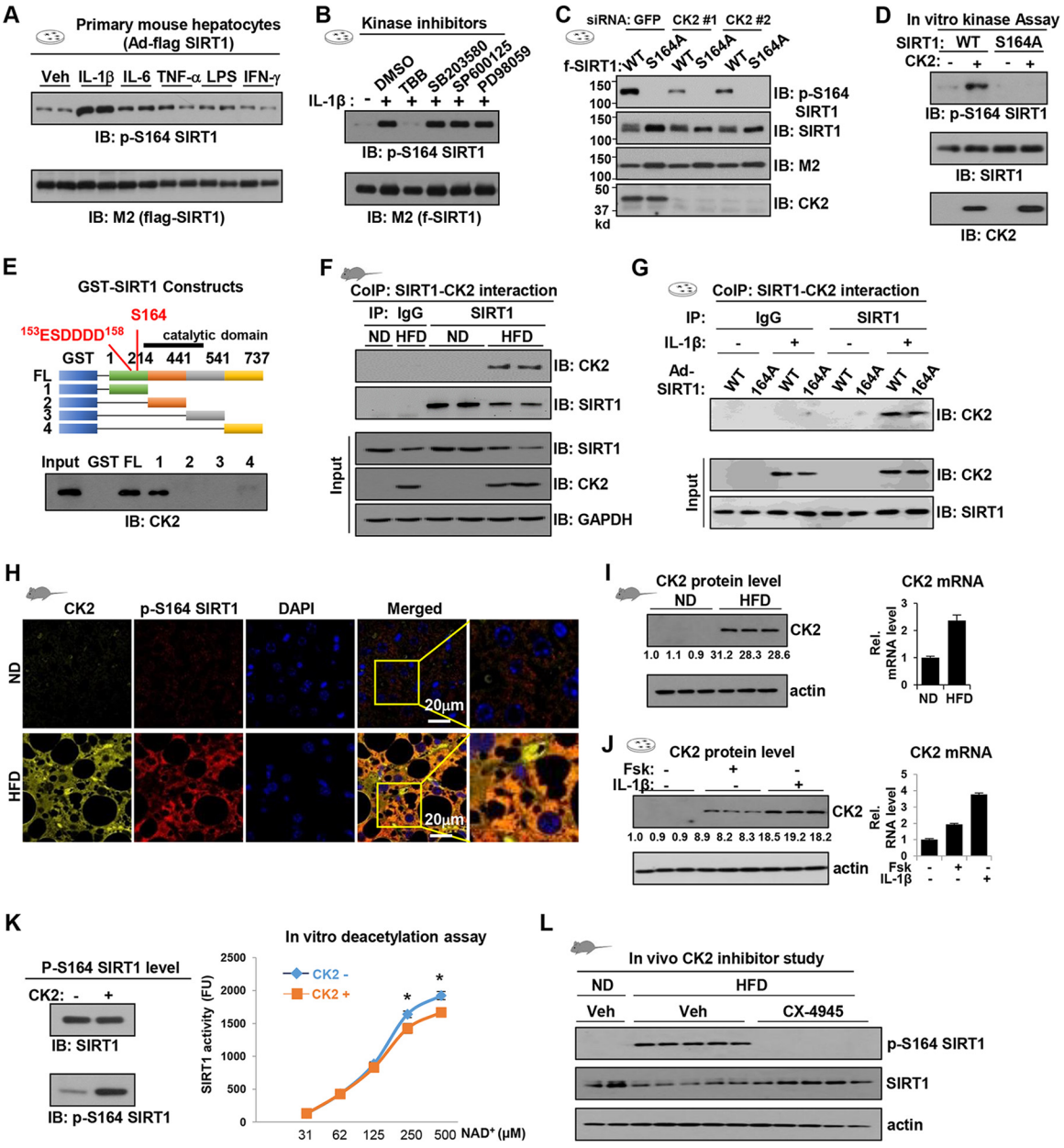

FIG 4 Obesity-induced CK2 mediates phosphorylation of SIRT1 at S164. (A) Primary mouse hepatocytes (PMH) were infected with Ad-Flag-SIRT1-WT and treated with cytokines as indicated for 1 h, and p-S164–SIRT1 and SIRT1 levels were measured by IB. Veh, vehicle; TNF-α, tumor necrosis factor alpha; IFN-γ, gamma interferon; LPS, lipopolysaccharide. (B) PMH were infected with Ad-Flag-SIRT1-WT; treated with TBB for CK2, SB203580 for mitogen-activated protein kinase, SP600125 for JNK, and PD98059 for MEK and then treated with IL-1β (10 ng/ml) for 1 h; and p-S164–SIRT1 levels were measured. DMSO, dimethyl sulfoxide. (C) PMH were transfected with two different siRNAs for CK2 or with control siRNAs for GFP. Twenty-four hours later, the cells were infected with Ad-Flag-SIRT1-WT or S164A, and 36 h later the cells were treated with IL-1β for 1 h and p-S164–SIRT1 levels were measured. (D) Immunoprecipitated Flag-SIRT1-WT or Flag-S164A-SIRT1, expressed in Cos-1 cells, was incubated with CK2, and p-S164–SIRT1 levels were detected. (E) CK2 interaction with GST fusion proteins containing different domains of SIRT1. Positions of S164 and the acidic cluster are shown. Bound CK2 was detected by IB. (F) Mice were fed an ND or HFD for 16 weeks, and the interaction of SIRT1 with CK2 was determined by CoIP using whole-cell liver extracts. (G) PMH were infected with adenovirus as indicated and treated with IL-1β, and interaction between SIRT1 and CK2 using whole-cell extracts was measured by CoIP. (H) Cellular localization of CK2 and p-S164–SIRT1 in liver sections from mice fed an ND or HFD diet for 16 weeks was examined by IF. (I and J) Hepatic protein (left) and mRNA (right) levels of CK2 in mice fed an ND or HFD for 16 weeks (I) or PMH treated with IL-1β or Fsk (10 μM) for 3 h (J) were determined. Below the CK2 protein blots, the CK2 levels relative to actin, with the first lane set to 1, are indicated. For the protein, 3 independent determinations are shown, and for mRNA, means ± SEM ($n = 3$) are shown. (K) Flag-SIRT1 was expressed in Cos-1 cells. (Left) Flag-SIRT1 immunoprecipitated from nuclear extracts by M2 agarose was incubated with CK2 *in vitro*, and SIRT1 and p-S164–SIRT1 levels were detected by IB. (Right) M2-agarose-bound Flag-SIRT1 then was washed with deacetylation buffer, and deacetylase activity was determined using fluorescently labeled Ac-p53 peptide ($n = 6$; results are means ± SEM; *, $P < 0.05$) as described in Materials and Methods. Statistical significance was determined by the Student *t* test. (L) Mice ($n = 5$/group) were fed an HFD for 16 weeks and then were treated with vehicle (Veh) or a CK2 inhibitor, CX-4945 (50 mg/kg of body weight), over a period of 40 days as previously described (28). Protein levels of endogenous SIRT1 and p-S164–SIRT1 in liver extracts were determined by IB. Normal levels of SIRT1 in livers from ND mice are shown for comparison.

To determine whether CK2 is a key regulator of SIRT1 phosphorylation status in diet-induced obese mice *in vivo*, p-S164–SIRT1 levels were measured in liver extracts of HFD mice that had been treated with an inhibitor of CK2, CX-4945 (28). Remarkably, p-S164–SIRT1 levels that were increased by feeding an HFD were undetectable in CX-4945-treated samples (Fig. 4L), demonstrating that CK2 is a key regulator of SIRT1 phosphorylation in diet-induced obese mice. These results indicate that obesity-induced CK2 mediates phosphorylation of SIRT1 at S164.

Obesity-linked S164-SIRT1 phosphorylation promotes pathological symptoms of liver steatosis. To investigate the functional consequences of obesity-induced phosphorylation of SIRT1 at S164, mice were fed an HFD, and Flag-SIRT1 WT, p-defective S164A-SIRT1, or p-mimic S164D-SIRT1 was adenovirally expressed in liver (Fig. 5A). As controls, mice fed an ND or HFD were infected with adenovirus-green fluorescent protein (Ad-GFP) control virus. Protein levels of Flag-SIRT1 WT and the S164 mutants in HFD mice were comparable among groups, and p-S164 SIRT1 was not detectable with the S164 mutants, as expected (Fig. 5B). Consistent with the nuclear localization studies in hepatocytes (Fig. 2D and E), the p-defective S164A mutant was detected nearly exclusively in the nucleus, and SIRT1 WT was predominantly nuclear with some cytoplasmic localization, whereas the p-mimic S164D mutant was detected largely in the cytoplasm in mouse liver (Fig. 5C).

Food intake and body weights were similar in all groups of HFD mice infected with Ad-SIRT1 WT or the S164 mutants (not shown). In contrast, the ratios of liver to body weights (Fig. 5D) and neutral lipid (Fig. 5E), liver TG (Fig. 5F), and liver cholesterol (not shown) levels all were reduced by expression of the p-defective S164A-SIRT1 compared to expression of the p-mimic S164D-SIRT1. Fatty liver is associated with insulin resistance and chronic inflammation (2, 3, 29). Fasting blood plasma levels of glucose, insulin, and the cytokines IL-6 and MCP1 were decreased (Fig. 5G), and glucose (Fig. 5H) and insulin tolerance (Fig. 5I) were also improved in the HFD mice expressing the S164A mutant compared to the S164D mutant. In transcriptional analysis, expression of hepatic genes involved in fatty acid oxidation was increased and expression of lipogenic and inflammatory genes was decreased in mice expressing SIRT1-WT or S164A-SIRT1, but these changes were largely absent from the p-mimic-S164D-SIRT1 mutant (Fig. 5J). Consistent with these results, treatment of hepatocytes with IL-1β decreased fatty acid oxidation gene expression and increased lipogenic gene expression, and cotreatment with the CK2 inhibitor, TBB, reversed these effects (not shown).

These results demonstrate that adenovirus-mediated expression of p-defective S164A-SIRT1 and, to a lesser extent, expression of WT SIRT1 but not the p-mimic S164D-SIRT1 reduce liver TG levels and improve glucose tolerance and serum profiles in HFD obese mice. These effects of phosphorylation of SIRT1 on lipid and glucose metabolism are consistent with a hypothesis that the elevated levels of SIRT1 phosphorylation at S164 observed in obese mice contribute to the symptoms of fatty liver.

S164-SIRT1 phosphorylation inhibits fatty acid oxidation and promotes fatty liver. To further examine the effects of SIRT1 phosphorylation on fatty liver symptoms in obese mice, we expressed WT SIRT1 and the p-mimic S164D-SIRT1 mutant in SIRT1-LKO mice to avoid possible confounding effects of endogenous hepatic SIRT1. Hepatic TG levels are regulated by multiple pathways, including fatty acid β-oxidation, lipogenesis, and lipoprotein uptake and secretion (2). Since liver-specific ablation of SIRT1 impaired β-oxidation in part by affecting the peroxisome proliferator-activated receptor alpha (PPARα)/PGC-1α pathway (19) and phosphorylation of SIRT1 at S164 inhibits its deacetylation of PGC-1α (Fig. 3C), we further investigated the effects of liver-specific expression of either SIRT1-WT or the p-mimic S164D mutant in SIRT1-LKO mice on fatty acid β-oxidation.

SIRT1-WT and S164D-SIRT1 levels were reconstituted by adenoviral expression in SIRT1-LKO mice fed an HFD (Fig. 6A, top) to normal physiological levels, similar to those in C57BL/6 mice fed an ND (Fig. 6A, bottom). Food intake, body weights, and adipose tissue weights were not notably changed by expression of SIRT1-WT or S164D-SIRT1 (not shown). SIRT1-LKO mice expressing SIRT1-WT had decreased liver-to-body-weight

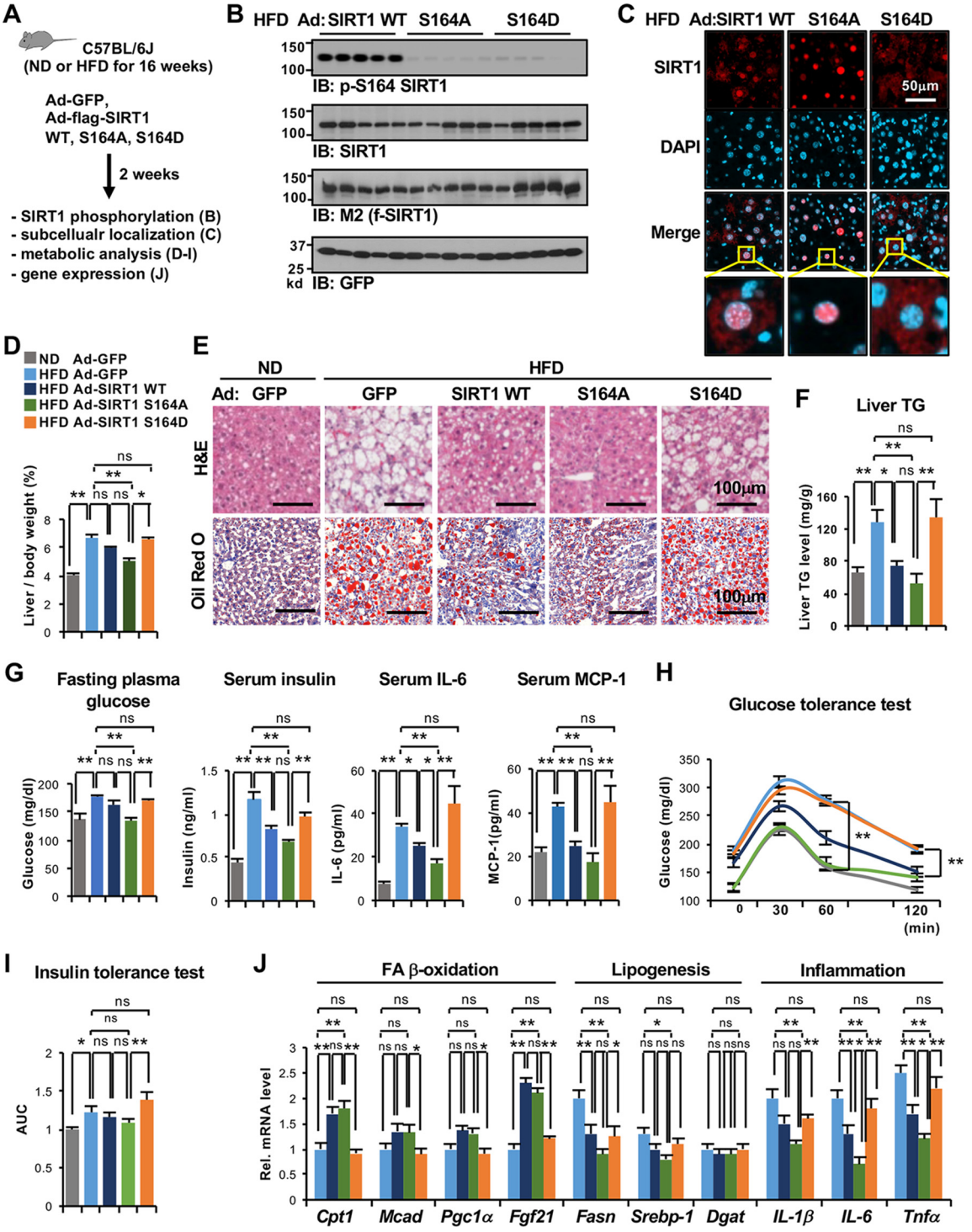

FIG 5 S164-SIRT1 phosphorylation promotes pathological symptoms of liver steatosis. (A) C57BL/6J male mice were fed an ND or HFD for 16 weeks and injected via the tail vein with adenoviruses as indicated, and 2 weeks later the mice were sacrificed for analyses. (B) Protein levels of SIRT1-WT or S164 mutants and GFP (an indicator of viral infection) and p-S164–SIRT1 in whole-cell liver extracts are shown. (C) SIRT1 in liver sections was detected by IF, and merged images of SIRT1 with nuclear 4′,6-diamidino-2-phenylindole (DAPI) staining are shown. The scale bars indicate 50 μm. (D) Liver/body weight ratios. (E) Liver sections stained with H&E and Oil Red O. (F) Liver TG levels. (G) Fasting plasma levels of glucose, insulin, IL-6, and MCP-1. (H) Plasma glucose levels at the indicated times after i.p. injection of glucose are shown. (I) Plasma glucose levels at the indicated times after i.p. injection of insulin were measured, and areas under the curve (AUC) are shown. (J) Hepatic mRNA levels of the indicated genes were measured by qRT-PCR. For panels D and F to J, data shown are means ± SEM (n = 5 mice/group); *, $P < 0.05$; **, $P < 0.01$; ns, statistically not significant. Statistical significance was determined by one-way ANOVA with Tukey's posttest.

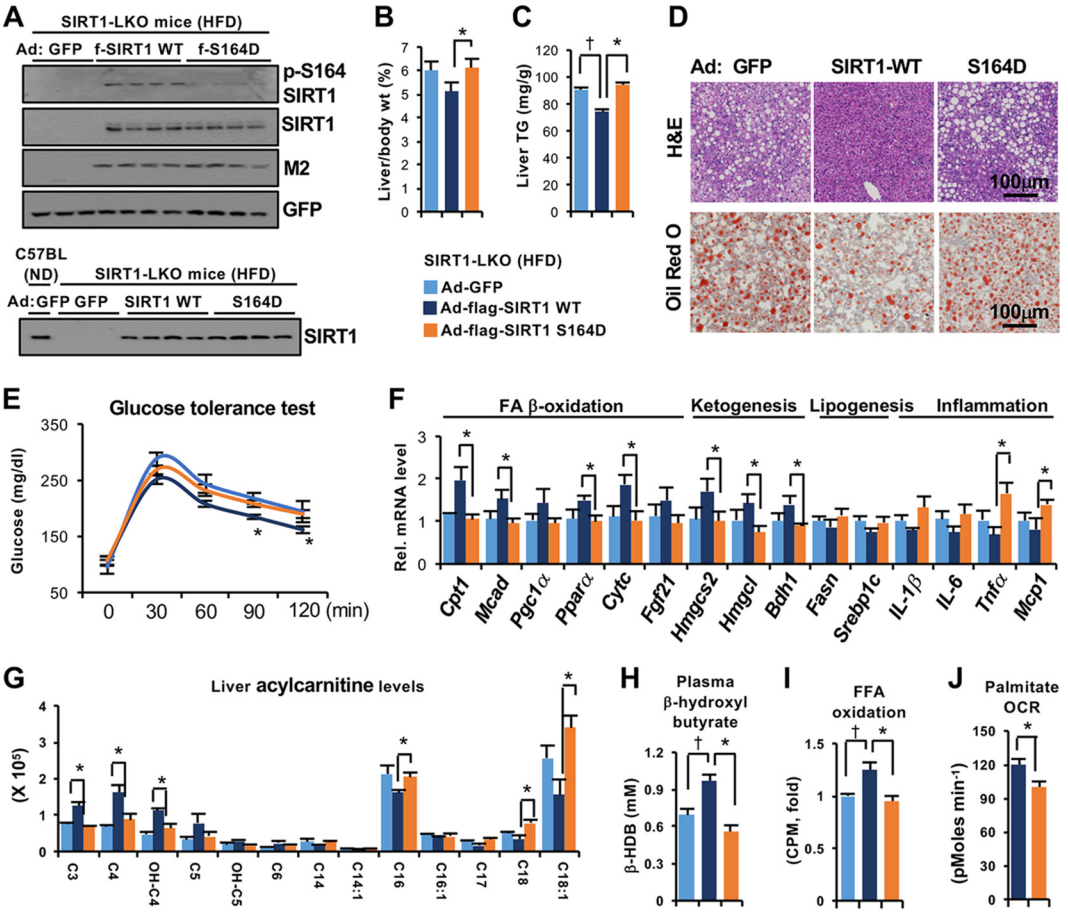

FIG 6 S164-SIRT1 phosphorylation inhibits β-oxidation and promotes liver steatosis. SIRT1-LKO mice fed an HFD for 6 weeks were infected with Ad-GFP, Ad-Flag-SIRT1-WT, or Ad-Flag-S164D-SIRT1 for 1 week. (A) Hepatic SIRT1 protein levels and p-S164–SIRT1 levels in SIRT1-LKO mice expressing SIRT1-WT or S164D-SIRT1 and control WT mice fed an ND (bottom) were determined by IB. (B) Relative liver weight as a percentage of total body weight ($n = 4$ mice/group). (C and D) Liver TG levels and liver sections stained with H&E and Oil Red O. (E) Plasma glucose levels at the indicated times after i.p. injection of glucose. (F) Hepatic mRNA levels of the indicated genes measured by qRT-PCR. (G and H) Serum β-hydroxyl butyrate and liver acylcarnitine levels determined by metabolomic analysis. (I and J) SIRT1-WT or S164D-SIRT1 was adenovirally expressed in primary mouse hepatocytes for 48 h, and palmitate oxidation (I) and the oxygen consumption rate (OCR) (J) were measured as described in Materials and Methods (means ± SEM; $n = 6$). Statistical significance was determined by one-way ANOVA with Tukey's posttest (B, C, and E to I) and by the Student t test (J).

ratios (Fig. 6B), liver TG levels (Fig. 6C), and liver neutral lipids detected by hematoxylin and eosin (H&E) and Oil Red O staining (Fig. 6D), but these effects were absent from mice expressing S164D-SIRT1. As expected from decreased liver TG levels, glucose tolerance was improved by expression of SIRT1-WT but not S164D-SIRT1 (Fig. 6E). In gene expression studies, mRNA levels of fat oxidation and ketogenic genes were increased and those of lipogenic and inflammatory genes were decreased with SIRT1-WT, but again, these effects were largely absent from S164D-SIRT1 (Fig. 6F).

Liver acylcarnitine levels, particularly long-chain species, are indicators of incomplete β-oxidation of fatty acids (30). Consistent with the results from gene expression studies, levels of long-chain acylcarnitine species were increased (Fig. 6G) and serum levels of a ketone body, β-hydroxyl butyrate (Fig. 6H), were decreased by expression of S164D-SIRT1 compared to SIRT1-WT. Further, palmitate oxidation and oxygen consumption rates were decreased with S164D-SIRT1 expression compared to SIRT1-WT in primary mouse hepatocytes (PMH) (Fig. 6I and J) and in human HepG2 cells (not shown). These results suggest that obesity-linked phosphorylation of SIRT1 leads to impaired β-oxidation and increased lipid accumulation in the liver, which contributes to pathological symptoms of NAFLD.

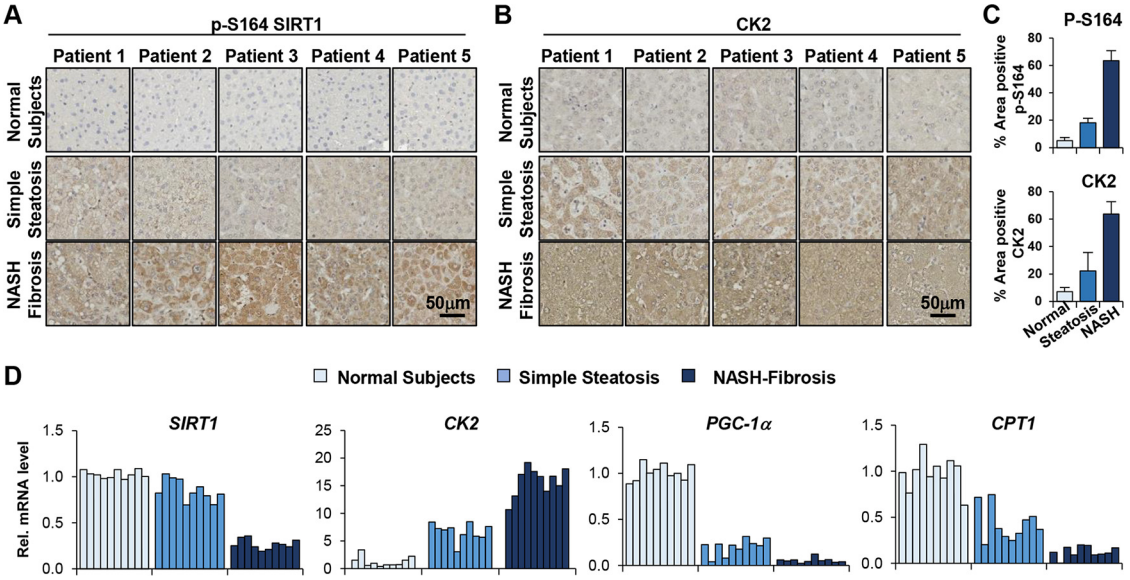

FIG 7 Phosphorylated p-S164–SIRT1 and CK2 protein levels and mRNA levels of key genes in NAFLD patients. (A to C) p-S164–SIRT1 and CK2 protein levels were detected by IHC in liver specimens of five healthy individuals or patients with either simple steatosis or severe NASH fibrosis. (C) Quantitation was determined using ImageJ software for stained tissues (ver.1.5; National Institutes of Health) according to the ImageJ user guide. (D) Hepatic mRNA levels of *SIRT1*, *CK2*, *PGC-1α*, and *CPT1*, in 10 healthy subjects and 10 simple steatosis or NASH fibrosis patients were measured by qRT-PCR.

p-S164–SIRT1 and CK2 levels are increased in livers of NAFLD patients. To determine whether the aberrant phosphorylation of SIRT1 by CK2 in obese mice was also observed in humans with fatty livers, we analyzed expression of p-S164–SIRT1 and CK2 in liver samples from healthy individuals and from NAFLD patients with either simple steatosis or severe NASH fibrosis. Protein levels of p-S164–SIRT1 and CK2 in liver sections, detected by IHC, were substantially increased in NASH patients and, to a lesser extent, in simple steatosis patients compared to healthy individuals (Fig. 7A to C). Hepatic mRNA levels of *CK2* were dramatically elevated in NASH patients, whereas those of *SIRT1*, *PGC-1α*, a key transcriptional coactivator promoting mitochondrial function, and *CPT1*, the rate-limiting protein in β-oxidation, were substantially decreased (Fig. 7D). Notably, the changes were intermediate in simple steatosis patients, indicating a correlation with disease severity. These results demonstrate that elevated levels of p-S164–SIRT1 and CK2 detected in obese mice are also elevated in liver samples of NAFLD patients and correlate with disease progression.

DISCUSSION

In this study, we show that SIRT1 is aberrantly phosphorylated at S164 in obesity by CK2, the expression of which is highly elevated in diet-induced obese mice and in NAFLD patients. This obesity-linked phosphorylation inhibits the nuclear localization of SIRT1, thus blocking SIRT1 function, and it also modestly inhibits SIRT1 activity. The decreased SIRT1 function in obesity contributes to impaired fatty acid oxidation and increased pathological symptoms of liver steatosis.

Compared to other sirtuins, SIRT1 has a long N-terminal domain that contains nuclear localization sequences (NLS) and sites for PTMs, including a site for JNK phosphorylation that promotes its degradation (9, 21, 31). In addition, this N-terminal domain of SIRT1 critically influences its deacetylase activity by interacting with STACs and proteins (22–24). Intriguingly, a single amino acid, human E230 (mE222), located in this region, is critical for activation of SIRT1 by all 117 of the tested STACs, including resveratrol (13). Further, expression of the SIRT1 N-terminal domain *trans*-activates SIRT1 deacetylase activity by interacting with endogenous SIRT1 and promoting interaction with its substrates, including NF-κB, and improved glucose regulation in mice (24). Based on the structural analysis of human SIRT1 (Fig. 2A), mouse S164 is located

near the m223-230 NLS and the functionally important mE222 residue. The negatively charged phosphorylated S164 may interact with the basic amino acid cluster (KRKKKRK) in the NLS, altering the conformation of the N-terminal domain and blocking interaction of the NLS with importin, which would explain the observed inhibition of nuclear localization of SIRT1 phosphorylated at S164. Changes in conformation near the functionally critical E230 residue could also affect SIRT1 interactions with STACs or with the substrates, reducing the deacetylase activity of SIRT1, as observed in the present study. Although both the nuclear localization and activity of SIRT1 are reduced by S164 phosphorylation, the relatively modest decrease in the intrinsic activity of SIRT1 phosphorylated by CK2 suggests that the major effect of the phosphorylation on the function of SIRT1 in cells is the inhibition of nuclear localization.

An unexpected finding in this study was the identification of CK2 as the kinase that mediates the aberrant phosphorylation of SIRT1 in obesity. Pharmacological inhibition of CK2 and siRNA-mediated downregulation of CK2, together with biochemical and imaging studies, provided evidence that CK2 directly interacts with and phosphorylates SIRT1 and that their interaction occurs in the cytoplasm of fatty livers in obese mice. CK2 directly interacts with target proteins through highly acidic amino acid clusters (25, 26), and intriguingly, an acidic amino acid E/D cluster adjacent to S164 in SIRT1 is conserved in nearly all vertebrates. In the present study, we show that hepatic expression of CK2 is dramatically elevated in HFD obese mice and in NAFLD patients, and the obesity-induced CK2 phosphorylates SIRT1 at S164 in the N-terminal domain and inhibits SIRT1 function. Since CK2 has multiple substrates in the liver, these studies suggest that increased phosphorylation of its substrates in obesity has other functional consequences. Future studies will be required to determine the mechanisms underlying the increased hepatic expression of CK2 in NAFLD and obesity as well as other CK2-mediated functions that may be altered in obesity.

CK2 was recently identified as a negative regulator of thermogenesis in beige fat cells in response to cAMP stimuli and to a high-fat diet (28). Remarkably, treatment with pharmacological inhibitors or antisense oligonucleotide-mediated downregulation of CK2 led to increases in energy expenditure and improved diet-induced obesity and insulin resistance. In mice with decreased CK2 function, liver TG levels were decreased and glucose regulation was improved. The similar metabolic responses to decreased CK2 activity (28) and the expression of the p-defective S164A-SIRT1 mutant in mice are consistent with our conclusion that phosphorylation of S164 by CK2 mediates the detrimental effects on hepatic lipid catabolism observed in diet-induced obese mice. In the present study, we found hepatic CK2 protein and mRNA levels were dramatically induced in HFD mice but, importantly, also in NAFLD patients, and CK2 expression levels correlated with disease severity in the patients, suggesting that these obesity-related changes observed in mice are also relevant in humans. Thus, combination treatment with an inhibitor of CK2 to block the obesity-linked phosphorylation of SIRT1 and SIRT1-activating compounds to reduce hepatic lipid levels may serve as an effective therapeutic option for treatment of NAFLD.

Signal-induced posttranslational modifications (PTMs) profoundly modulate the function of many regulatory proteins in response to environmental cues (32–35). SIRT1 has also been shown to be a target of numerous PTMs, including phosphorylation by JNK, CDK1, and AMPK, that affect its activity (31, 35–37). For example, a recent study showed that SIRT1 is phosphorylated by AMPK and that this phosphorylation increases SIRT1 deacetylation in regulation of p53 (36). PTMs of proteins, including SIRT1, have been extensively studied, but *in vivo* physiological and pathological functions of PTMs are still poorly understood. While the manuscript was under revision, a knock-in mouse study showed that phosphorylation of T522 is critical for tissue-specific modulation of SIRT1 function in energy metabolism in adipose tissue and liver *in vivo* (38). In the present study, we have demonstrated that S164 phosphorylation of SIRT1 by CK2 is linked to obesity and further elucidated the mechanisms by which phosphorylation at a single-amino-acid residue inhibits SIRT1 function, resulting in impaired fatty acid oxidation and promotion of fatty liver and glucose intolerance. Targeting such disease-

related PTM sites therapeutically might be more selective than inhibition of the overall function of a protein, resulting in fewer side effects, as suggested in recent studies targeting obesity-linked PPARγ phosphorylation (39, 40). Thus, inhibition of phosphorylated S164-SIRT1 and CK2 may serve as a new therapeutic approach for treatment of NAFLD and diabetes and other obesity-related disease.

MATERIALS AND METHODS

Materials. Antibody for SIRT1 (07-131) was from Millipore, antibody for pan-p-Ser (ab9232) was from Abcam, antibodies for acetyl-Lys (9441S) and actin (4957S) were from Cell Signaling, and those for lamin (sc-20680), tubulin (sc-5274), PGC-1α (sc-13067), SREBP-1 (sc-8984), CK2 (sc-12738), and GFP (sc-8334) were from Santa Cruz Biotechnology. M2 antibody, M2 agarose, tryptic soy agar (TSA), NAD^+, nicotinamide (NAM), and kinase inhibitors were from Sigma-Aldrich, Inc., and IL-1β was from R&D Systems. The p-S164–SIRT1 antibody was custom developed by Abmart, Inc. A 1:20,000 dilution of the antibody selectively detected SIRT1-WT compared to the phosphorylation-defective S164A-SIRT1 mutant (not shown). Purified CK2 was obtained from New England BioLabs, Inc., and siRNAs for CK2 and GFP were from Bioneer, Inc. (Seoul, South Korea). Mouse SIRT1 cDNA was used for the expression of WT and mutant SIRT1.

Animal experiments. For a dietary obese mouse model, C57BL/6J male mice were fed a high-fat diet (HFD) (60% fat) for 12 to 16 weeks. Since SIRT1-LKO mice show impaired fatty acid β-oxidation and increased inflammation upon HFD challenge (19), these mice were fed an HFD for 6 weeks. For expression of SIRT1 and mutants, recombinant adenovirus was used for hepatic studies, because adenovirus-mediated expression of proteins is largely confined to the liver (41). Adenovirus (2.5×10^8 to 5.0×10^8 active viral particles in 100 μl saline) expressing SIRT1-WT or S164 mutants was injected via the tail vein, and 1 to 2 week later livers were collected. Injection of these viral doses does not cause inflammation (32, 33). For the glucose tolerance test, mice were fasted overnight and injected intraperitoneally (i.p.) with 2 g/kg of body weight glucose (Sigma-Aldrich Inc.). For the insulin tolerance test, mice were fasted for 5 to 6 h and injected i.p. with 1 U/kg insulin (Lilly, Inc.), and blood plasma glucose levels were measured. Plasma insulin and cytokine levels were measured by enzyme-linked immunosorbent assay (ELISA) from R&D Systems, and liver acylcarnitine and serum hydroxyl butyrate levels were measured in the University of Illinois Metabolomics Facility. For *in vivo* CK2 inhibitor experiments, we used liver samples from C57BL6 mice that had been fed HFD for 16 weeks and were treated with vehicle or a CK2 inhibitor, CX-4945 (50 mg/kg body weight), over a period of 40 days as previously described (28). All animal use and adenoviral protocols were approved by the Institutional Animal Use and Care and Biosafety Committees.

LC-MS/MS proteomic analysis. Ad-Flag-mouse SIRT1 was injected via the tail vein in mice, and 1 week later, Flag-SIRT1 in whole-cell liver extracts was purified by binding to M2 agarose and subjected to proteomic analysis as described in our previous studies (12, 34). MS/MS spectra were screened against the SIRT1 sequence using SEQUEST (Thermo Finnigan), and the identified phosphorylated peptides were further confirmed by manual inspection of the MS2 and MS3 spectra.

Microscopy. Primary SIRT1, CK2, and p-S164 antibodies were detected with horseradish peroxidase (HRP)/DAB IHC detection kits (Abcam), and sections were imaged with a NanoZoomer scanner. Frozen liver sections were stained with Oil Red O, and paraffin-embedded sections were stained with H&E. For IF, Alexa Fluor 594- and 647-conjugated secondary antibodies were used and sections were imaged by confocal microscopy (Zeiss LSM 700).

Subcellular fractionation. Liver tissues were minced, resuspended in hypotonic buffer, and homogenized with a Dounce homogenizer. The nuclear pellet and cytoplasmic supernatant were collected after centrifugation as previously described (42, 43), and fractionation was monitored by measuring lamin and tubulin protein levels.

***In vitro* kinase assay.** Immunoprecipitated Flag-SIRT1 protein, expressed in Cos-1 cells, was incubated in kinase buffer (25 mM Tris [pH 7.5], 5 mM β-glycerophosphate, 2 mM dithiothreitol [DTT], 0.1 mM Na_3VO_4, 0.025% bovine serum albumin [BSA]) with 20 μM ATP and 20 ng of CK2 at 30°C for 30 min, and p-S164–SIRT1 levels were measured by immunoblotting (IB).

***In vitro* Fluor-De-Lys deacetylation assays.** Flag-SIRT1 and Flag-SIRT1 mutants were expressed in Cos-1 cells and immunoprecipitated with M2 agarose from whole-cell or nuclear extracts, and the level of phosphorylation of SIRT1 at S164 was determined by IB as indicated in the figure legends. The immunoprecipitated Flag-SIRT1 proteins were incubated with fluorescent Ac-p53 peptide (CS1040; Sigma, Inc.) and increasing concentrations of NAD^+ in 50 mM Tris-Cl (pH 8.0), 137 mM NaCl, 2.7 mM KCl, 1 mM $MgCl_2$, 1 mg/ml BSA for 45 min at 30°C, and the deacetylase activity was determined by measuring fluorescent emission at 460 nm following excitation at 360 nm according to the manufacturer's instructions.

***In vitro* histone deacetylation assays.** Histone H3 was acetylated by incubation with purified p300 and acetyl-coenzyme A in acetylation buffer (50 mM HEPES, pH 7.9, 10% glycerol). After incubation at 30°C for 30 min, the beads were thoroughly washed, and acetylated histone H3 was incubated with the immunoprecipitated Flag-SIRT1 proteins in deacetylation buffer (Tris-HCl, pH 8.8, 5% glycerol, 50 mM NaCl, 4 mM $MgCl_2$, 1 mM DTT, and 50 μM NAD^+) at 37°C for 1 h, and levels of acetylated histone H3 and total histone H3 were measured by IB analysis using histone H3K9/14-Ac antibody and H3 antibody, respectively.

In-cell deacetylation assay. Cos-1 cells were cotransfected with plasmids for SREBP-1c or PGC-1α, together with p300 and either SIRT1-WT or the S164 mutants. The cells were treated with 500 nM TSA

and 10 mM NAM for 6 h and harvested. Acetylation levels of PGC-1α and SREBP-1c were detected by the IP/IB method as described in our previous studies (12, 32, 34).

Isolation of primary mouse hepatocytes. Hepatocytes were isolated by collagenase (0.8 mg/ml; Sigma-Aldrich Co.) perfusion through the portal vein of mice anesthetized with isoflurane. The hepatocyte suspension was filtered through a cell strainer (100-μm nylon; BD), washed with M199 medium (M4530; Sigma), resuspended in M199 medium, and centrifuged through 45% Percoll (Sigma-Aldrich Inc.).

Measurement of oxygen consumption rate in PMH. PMH were infected with Ad-SIRT1 or Ad-S164D-SIRT1 and treated with palmitic acid (2 mM). Cells were further treated at 30-min intervals with oligomycin (14 μM), the pharmacological uncoupler FCCP (10 μM), or the complex I and III inhibitor antimycin A (4 μM). The oxygen consumption rate was measured with an XF Analyzer (Seahorse Bioscience, Inc.) as described previously (44).

Downregulation of CK2 in PMH. PMH were transfected with siRNA for CK2 or control GFP siRNA (5 nmol). Twenty-four hours later, the cells were infected with adenoviral vectors, and 36 to 48 h later, they were further treated with IL-1β for 1 h and harvested for further analyses.

GST pulldown, CoIP, and qRT-PCR. GST-SIRT1 fusion proteins expressed in bacteria were purified and incubated with purified CK2, and CK2 bound to the GST-SIRT1 proteins was detected by IB. CoIP assays were done as previously described (12, 32, 34). Dilutions of 1:20,000 for the p-S164 SIRT1 antibody or 1 μg of SIRT antibody were used. Briefly, 0.25 to 0.5 mg of whole-cell mouse liver extracts were incubated with antibody at 4°C overnight. The immune complex was isolated by incubation with protein G-agarose, and proteins in the immunoprecipitates were detected by IB. For quantitative reverse transcription-PCR (qRT-PCR) analyses, mRNA levels were normalized to 36B4 mRNA levels.

NAFLD patient study. Liver specimens from 10 unidentifiable healthy individuals or from mild simple steatosis or severe NASH fibrosis NAFLD patients were obtained from the Liver Tissue Procurement and Distribution System. Proteins levels were detected by IHC and mRNA levels by qRT-PCR. The IHC quantitation was performed using ImageJ software for stained tissues (ver. 1.5; National Institutes of Health).

Statistical analysis. Statistical significance was determined by Student's two-tailed *t* test or one-way analysis of variance (ANOVA) with Tukey's posttest as appropriate. *P* values of <0.05 were considered statistically significant.

SUPPLEMENTAL MATERIAL

Supplemental material for this article may be found at https://doi.org/10.1128/MCB.00006-17.

SUPPLEMENTAL FILE 1, PDF file, 0.1 MB.

ACKNOWLEDGMENTS

We thank the Liver Tissue Procurement and Distribution System of the NIH for providing human liver specimens. We also thank Shwu-Yuan Wu and Cheng-Ming Chiang for providing purified p300 and Mark Leid for GST-SIRT1 constructs.

This study was supported by a National Research Foundation of Korea grant, NRF-2013-013774 to S.E.C., and an American Diabetes Association Innovative Basic Science Award (1-16-IBS-156) and National Institutes of Health grants, DK62777 and DK95842, to J.K.K.

S. E. Choi, S. Kwon, S. Seok, and J. K. Kemper designed the research; S. E. Choi, S. Kwon, S. Seok, and Z. Xiao performed experiments; K.-W. Lee, Y. Kang, X. Li, K. Shinoda, and S. Kajimura provided key materials and expertise in *in vivo* studies; S. E. Choi, S. Kwon, S. Seok, Z. Xiao, B. Kemper, and J. K. Kemper analyzed data; and S. E. Choi, S. Kwon, S. Seok, B. Kemper, and J. K. Kemper wrote the paper.

We have no conflicts of interest to declare.

REFERENCES

1. Eckel RH, Grundy SM, Zimmet PZ. 2005. The metabolic syndrome. Lancet 365:1415–1428. https://doi.org/10.1016/S0140-6736(05)66378-7.
2. Cohen JC, Horton JD, Hobbs HH. 2011. Human fatty liver disease: old questions and new insights. Science 332:1519–1523. https://doi.org/10.1126/science.1204265.
3. Loomba R, Sanyal AJ. 2013. The global NAFLD epidemic. Nat Rev Gastroenterol Hepatol 10:686–690.
4. Guarente L. 2011. Sirtuins, aging, and metabolism. Cold Spring Harbor Symp Quant Biol 76:81–90. https://doi.org/10.1101/sqb.2011.76.010629.
5. Imai S, Guarente L. 2010. Ten years of NAD-dependent SIR2 family deacetylases: implications for metabolic diseases. Trends Pharmacol Sci 31:212–220. https://doi.org/10.1016/j.tips.2010.02.003.
6. Canto C, Auwerx J. 2009. Caloric restriction, SIRT1 and longevity. Trends Endocrinol Metab 20:325–331. https://doi.org/10.1016/j.tem.2009.03.008.
7. Finkel T, Deng CX, Mostoslavsky R. 2009. Recent progress in the biology and physiology of sirtuins. Nature 460:587–591. https://doi.org/10.1038/nature08197.
8. Kemper JK, Choi SE, Kim DH. 2013. Sirtuin 1 deacetylase: a key regulator of hepatic lipid metabolism. Vitam Horm 91:385–404. https://doi.org/10.1016/B978-0-12-407766-9.00016-X.
9. Haigis MC, Sinclair DA. 2010. Mammalian sirtuins: biological insights and disease relevance. Annu Rev Pathol 5:253–295. https://doi.org/10.1146/annurev.pathol.4.110807.092250.
10. Rodgers JT, Lerin C, Haas W, Gygi SP, Spiegelman BM, Puigserver P. 2005.

Nutrient control of glucose homeostasis through a complex of PGC-1alpha and SIRT1. Nature 434:113–118.
11. Rodgers JT, Puigserver P. 2007. Fasting-dependent glucose and lipid metabolic response through hepatic sirtuin 1. Proc Natl Acad Sci U S A 104:12861–12866. https://doi.org/10.1073/pnas.0702509104.
12. Ponugoti B, Kim DH, Xiao Z, Smith Z, Miao J, Zang M, Wu SY, Chiang CM, Veenstra TD, Kemper JK. 2010. SIRT1 deacetylates and inhibits SREBP-1C activity in regulation of hepatic lipid metabolism. J Biol Chem 285: 33959–33970. https://doi.org/10.1074/jbc.M110.122978.
13. Hubbard BP, Gomes AP, Dai H, Li J, Case AW, Considine T, Riera TV, Lee JE, E Sy, Lamming DW, Pentelute BL, Schuman ER, Stevens LA, Ling AJ, Armour SM, Michan S, Zhao H, Jiang Y, Sweitzer SM, Blum CA, Disch JS, Ng PY, Howitz KT, Rolo AP, Hamuro Y, Moss J, Perni RB, Ellis JL, Vlasuk GP, Sinclair DA. 2013. Evidence for a common mechanism of SIRT1 regulation by allosteric activators. Science 339:1216–1219. https://doi.org/10.1126/science.1231097.
14. Sinclair DA, Guarente L. 2014. Small-molecule allosteric activators of sirtuins. Annu Rev Pharmacol Toxicol 54:363–380. https://doi.org/10.1146/annurev-pharmtox-010611-134657.
15. Canto C, Houtkooper RH, Pirinen E, Youn DY, Oosterveer MH, Cen Y, Fernandez-Marcos PJ, Yamamoto H, Andreux PA, Cettour-Rose P, Gademann K, Rinsch C, Schoonjans K, Sauve AA, Auwerx J. 2012. The NAD(+) precursor nicotinamide riboside enhances oxidative metabolism and protects against high-fat diet-induced obesity. Cell Metab 15:838–847. https://doi.org/10.1016/j.cmet.2012.04.022.
16. Yoshino J, Mills KF, Yoon MJ, Imai S. 2011. Nicotinamide mononucleotide, a key NAD(+) intermediate, treats the pathophysiology of diet- and age-induced diabetes in mice. Cell Metab 14:528–536. https://doi.org/10.1016/j.cmet.2011.08.014.
17. Canto C, Auwerx J. 2012. Targeting sirtuin 1 to improve metabolism: all you need is NAD(+)? Pharmacol Rev 64:166–187. https://doi.org/10.1124/pr.110.003905.
18. Pfluger PT, Herranz D, Velasco-Miguel S, Serrano M, Tschop MH. 2008. Sirt1 protects against high-fat diet-induced metabolic damage. Proc Natl Acad Sci U S A 105:9793–9798. https://doi.org/10.1073/pnas.0802917105.
19. Purushotham A, Schug TT, Xu Q, Surapureddi S, Guo X, Li X. 2009. Hepatocyte-specific deletion of SIRT1 alters fatty acid metabolism and results in hepatic steatosis and inflammation. Cell Metab 9:327–338. https://doi.org/10.1016/j.cmet.2009.02.006.
20. Cao D, Wang M, Qiu X, Liu D, Jiang H, Yang N, Xu RM. 2015. Structural basis for allosteric, substrate-dependent stimulation of SIRT1 activity by resveratrol. Genes Dev 29:1316–1325. https://doi.org/10.1101/gad.265462.115.
21. Tanno M, Sakamoto J, Miura T, Shimamoto K, Horio Y. 2007. Nucleocytoplasmic shuttling of the NAD+-dependent histone deacetylase SIRT1. J Biol Chem 282:6823–6832. https://doi.org/10.1074/jbc.M609554200.
22. Kim EJ, Kho JH, Kang MR, Um SJ. 2007. Active regulator of SIRT1 cooperates with SIRT1 and facilitates suppression of p53 activity. Mol Cell 28:277–290. https://doi.org/10.1016/j.molcel.2007.08.030.
23. Atkins KM, Thomas LL, Barroso-Gonzalez J, Thomas L, Auclair S, Yin J, Kang H, Chung JH, Dikeakos JD, Thomas G. 2014. The multifunctional sorting protein PACS-2 regulates SIRT1-mediated deacetylation of p53 to modulate p21-dependent cell-cycle arrest. Cell Rep 8:1545–1557. https://doi.org/10.1016/j.celrep.2014.07.049.
24. Ghisays F, Brace CS, Yackly SM, Kwon HJ, Mills KF, Kashentseva E, Dmitriev IP, Curiel DT, Imai SI, Ellenberger T. 2015. The N-terminal domain of SIRT1 is a positive regulator of endogenous SIRT1-dependent deacetylation and transcriptional outputs. Cell Rep 10:1665–1673. https://doi.org/10.1016/j.celrep.2015.02.036.
25. Kang H, Jung JW, Kim MK, Chung JH. 2009. CK2 is the regulator of SIRT1 substrate-binding affinity, deacetylase activity and cellular response to DNA-damage. PLoS One 4:e6611. https://doi.org/10.1371/journal.pone.0006611.
26. Scott GK, Fei H, Thomas L, Medigeshi GR, Thomas G. 2006. A PACS-1, GGA3 and CK2 complex regulates CI-MPR trafficking. EMBO J 25: 4423–4435. https://doi.org/10.1038/sj.emboj.7601336.
27. Lumeng CN, Saltiel AR. 2011. Inflammatory links between obesity and metabolic disease. J Clin Investig 121:2111–2117. https://doi.org/10.1172/JCI57132.
28. Shinoda K, Ohyama K, Hasegawa Y, Chang HY, Ogura M, Sato A, Hong H, Hosono T, Sharp LZ, Scheel DW, Graham M, Ishihama Y, Kajimura S. 2015. Phosphoproteomics identifies CK2 as a negative regulator of beige adipocyte thermogenesis and energy expenditure. Cell Metab 22: 997–1008. https://doi.org/10.1016/j.cmet.2015.09.029.
29. Perry RJ, Samuel VT, Petersen KF, Shulman GI. 2014. The role of hepatic lipids in hepatic insulin resistance and type 2 diabetes. Nature 510: 84–91. https://doi.org/10.1038/nature13478.
30. Koves TR, Ussher JR, Noland RC, Slentz D, Mosedale M, Ilkayeva O, Bain J, Stevens R, Dyck JR, Newgard CB, Lopaschuk GD, Muoio DM. 2008. Mitochondrial overload and incomplete fatty acid oxidation contribute to skeletal muscle insulin resistance. Cell Metab 7:45–56. https://doi.org/10.1016/j.cmet.2007.10.013.
31. Gao Z, Zhang J, Kheterpal I, Kennedy N, Davis RJ, Ye J. 2011. Sirtuin 1 (SIRT1) protein degradation in response to persistent c-Jun N-terminal kinase 1 (JNK1) activation contributes to hepatic steatosis in obesity. J Biol Chem 286:22227–22234. https://doi.org/10.1074/jbc.M111.228874.
32. Kim DH, Xiao Z, Kwon S, Sun X, Ryerson D, Tkac D, Ma P, Wu SY, Chiang CM, Zhou E, Xu HE, Palvimo JJ, Chen LF, Kemper B, Kemper JK. 2015. A dysregulated acetyl/SUMO switch of FXR promotes hepatic inflammation in obesity. EMBO J 34:184–199. https://doi.org/10.15252/embj.201489527.
33. Kim DH, Kwon S, Byun S, Xiao Z, Park S, Wu SY, Chiang CM, Kemper B, Kemper JK. 2016. Critical role of RanBP2-mediated SUMOylation of Small Heterodimer Partner in maintaining bile acid homeostasis. Nat Commun 7:12179. https://doi.org/10.1038/ncomms12179.
34. Kemper JK, Xiao Z, Ponugoti B, Miao J, Fang S, Kanamaluru D, Tsang S, Wu S, Chiang CM, Veenstra TD. 2009. FXR acetylation is normally dynamically regulated by p300 and SIRT1 but constitutively elevated in metabolic disease states. Cell Metab 10:392–404. https://doi.org/10.1016/j.cmet.2009.09.009.
35. Kwon HS, Ott M. 2008. The ups and downs of SIRT1. Trends Biochem Sci 33:517–525. https://doi.org/10.1016/j.tibs.2008.08.001.
36. Lau AW, Liu P, Inuzuka H, Gao D. 2014. SIRT1 phosphorylation by AMP-activated protein kinase regulates p53 acetylation. Am J Cancer Res 4:245–255.
37. Sasaki T, Maier B, Koclega KD, Chruszcz M, Gluba W, Stukenberg PT, Minor W, Scrable H. 2008. Phosphorylation regulates SIRT1 function. PLoS One 3:e4020. https://doi.org/10.1371/journal.pone.0004020.
38. Lu J, Xu Q, Ji M, Guo X, Xu X, Fargo DC, Li X. 2017. The phosphorylation status of T522 modulates tissue-specific functions of SIRT1 in energy metabolism in mice. EMBO Rep 18:841–857. https://doi.org/10.15252/embr.201643803.
39. Choi JH, Banks AS, Estall JL, Kajimura S, Bostrom P, Laznik D, Ruas JL, Chalmers MJ, Kamenecka TM, Bluher M, Griffin PR, Spiegelman BM. 2010. Anti-diabetic drugs inhibit obesity-linked phosphorylation of PPARgamma by Cdk5. Nature 466:451–456. https://doi.org/10.1038/nature09291.
40. Banks AS, McAllister FE, Camporez JP, Zushin PJ, Jurczak MJ, Laznik-Bogoslavski D, Shulman GI, Gygi SP, Spiegelman BM. 2015. An ERK/Cdk5 axis controls the diabetogenic actions of PPARgamma. Nature 517: 391–395. https://doi.org/10.1038/nature13887.
41. Connelly S, Mech C. 2004. Delivery of adenoviral DNA to mouse liver. Methods Mol Biol (Clifton, NJ) 246:37–52.
42. Seok S, Fu T, Choi SE, Li Y, Zhu R, Kumar S, Sun X, Yoon G, Kang Y, Zhong W, Ma J, Kemper B, Kemper JK. 2014. Transcriptional regulation of autophagy by an FXR-CREB axis. Nature 516:108–111.
43. Seok S, Kanamaluru D, Xiao Z, Ryerson D, Choi SE, Suino-Powell K, Xu HE, Veenstra TD, Kemper JK. 2013. Bile acid signal-induced phosphorylation of small heterodimer partner by protein kinase Czeta is critical for epigenomic regulation of liver metabolic genes. J Biol Chem 288: 23252–23263. https://doi.org/10.1074/jbc.M113.452037.
44. Fu T, Seok S, Choi S, Huang Z, Suino-Powell K, Xu HE, Kemper B, Kemper JK. 2014. MicroRNA 34a inhibits beige and brown fat formation in obesity in part by suppressing adipocyte fibroblast growth factor 21 signaling and SIRT1 function. Mol Cell Biol 34:4130–4142. https://doi.org/10.1128/MCB.00596-14.